DOI: 10.1002/anie.201003213

Nanotechnology

Uniform Hollow Carbon Shells: Nanostructured Graphitic Supports for Improved Oxygen-Reduction Catalysis**

*Zachary L. Schaefer, Matthew L. Gross, Michael A. Hickner, and Raymond E. Schaak**

Nanostructured high-surface-area carbon materials are ubiquitous in many applications, including catalysis, energy storage, and separations.[1–3] As supports for catalytic nanoparticles, nanostructured carbons can provide conductive substrates with high surface areas and excellent dispersion characteristics, which are important both for optimizing the synergistic nanoparticle–support interactions and for maximizing the mass activity of expensive precious metal catalysts.[4,5] This is particularly important for platinum-based nanoparticle catalysts, the benchmark electrocatalysts for proton-exchange-membrane fuel cells (PEMFC) that facilitate hydrogen oxidation at the anode and the oxygen reduction reaction (ORR) at the cathode.[6] The ORR is critically important for fuel-cell applications because it is the reaction that prevents maximum efficiency from being realized.[7] General strategies for improving ORR catalysis focus on increasing the accessible surface area of the catalyst and enhancing activity by size reduction, nanostructure control, and alloying.[8–10]

Herein, we describe a significant improvement in apparent platinum mass activity for the ORR in 0.5 M H_2SO_4 by anchoring platinum nanoparticles (Pt NPs) onto a new type of nano-engineered carbon support: monodisperse spherical nanoshells of graphitic carbon that are intermediate in size between C_{60} and most other hollow graphitic nanomaterials. Nanostructured carbon materials are often prepared by carbon replication of sacrificial colloidal and porous templates,[1,2,11] chemical leaching of metals from metal carbides,[12] pyrolysis of carbon-rich organic materials,[1] and a variety of other methods.[13] For all of these methods, high-temperature (> 600 °C) processing is typically required to produce graphitic carbon.[12]

Our approach to graphitic carbon nanoshells, shown schematically in Figure 1, is inspired by carbide-derived carbons (CDCs), which are formed by high-temperature/high-pressure extraction of non-carbon elements from metal carbides.[12] For example, silicon and titanium can be leached

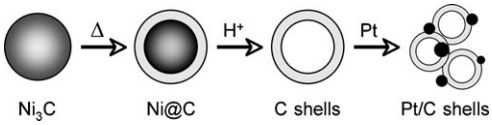

Figure 1. Multistep reaction pathway for synthesizing hollow carbon shells and Pt/C shell catalysts using Ni_3C nanoparticle precursors.

from SiC and TiC, respectively, using chlorine gas. The leaching process introduces large numbers of micropores and mesopores, which result in high surface areas. However, the high temperatures and large particle sizes make it difficult to exploit CDCs as highly-dispersible supports for catalytic nanoparticles. Our nanostructure design strategy (Figure 1) yields highly dispersible uniform nanoshells of graphitic carbon with high surface areas by synergistically merging several important materials capabilities from colloidal nanoscience and solid-state chemistry. Recent reports have described the synthesis of nanocrystalline Ni_3C[14] and NPs of the hcp allotrope of nickel,[15] both of which have similar XRD patterns. The product of a reaction claimed to yield near-monodisperse particles of hcp Ni,[15] when heated, behaves as would be expected for Ni_3C, decomposing at about 420 °C.[16] In nanoparticle form, this decomposition results in phase separation to generate a nickel core surrounded by a carbon shell. Transition metals are known to catalyze the low-temperature graphitization of carbon,[17] which leads to a graphitic carbon shell. Finally, nickel metal is readily soluble in HNO_3, so it can be removed to leave behind uniform colloidal shells of graphitic carbon that were templated by the Ni_3C NP precursors.

Powder XRD data (Figure 2) confirms the formation of Ni_3C NPs, which serve as the precursor to the hollow carbon shells. (Our ability to extract carbon from this phase, which has previously been attributed to hcp Ni,[15] provides further evidence that it is most likely Ni_3C and not the metastable hcp allotrope of nickel.) Figure 3a shows a TEM image of the colloidal Ni_3C NPs, which are (19 ± 3 nm) in diameter. A high-resolution TEM (HRTEM) image of a phase-separated nickel-core carbon-shell (Ni@C) particle formed after heating to 450 °C under argon is shown in Figure 3b. The nickel core exhibits lattice fringes of 2.0 Å, which correspond to the (111) plane of fcc Ni. The carbon shell, which has a thickness that

[*] Z. L. Schaefer, Prof. R. E. Schaak
Department of Chemistry and Materials Research Institute
The Pennsylvania State University
University Park, PA 16802 (USA)
E-mail: schaak@chem.psu.edu
M. L. Gross, Prof. M. A. Hickner
Department of Materials Science and Engineering, The Pennsylvania State University
University Park, PA 16802 (USA)

[**] This work was supported by the U.S. Department of Energy (DE-FG02-08ER46483). TEM imaging was performed in the Electron Microscopy Facility of the Huck Institutes of the Life Sciences and at the Materials Characterization Lab at the Penn State Materials Research Institute. The authors thank Dr. Joe Kulik (Penn State University) for acquiring the HRTEM images and Prof. Daniel Shantz (Texas A&M University) for N_2 adsorption measurements.
Supporting information for this article is available on the WWW under http://dx.doi.org/10.1002/anie.201003213.

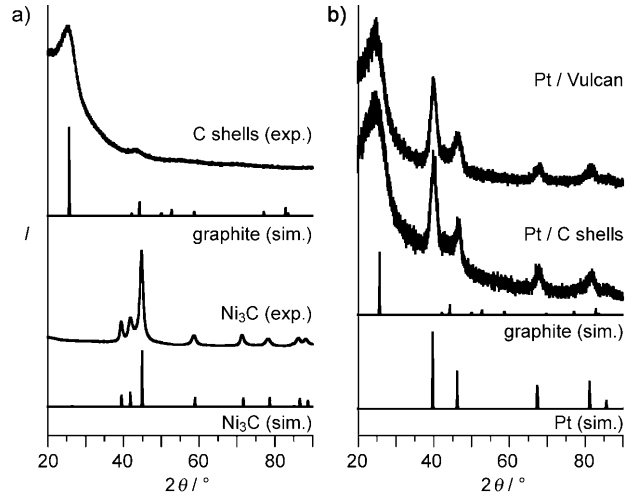

Figure 2. Powder XRD patterns for a) Ni_3C nanoparticle precursor (as-synthesized) and the carbon-shell products, and b) polyol-deposited 5 wt% Pt/C shell and 5 wt% Pt/Vulcan supported nanoparticle catalysts. Simulated XRD patterns for Ni_3C, graphite, and platinum are shown for comparison.

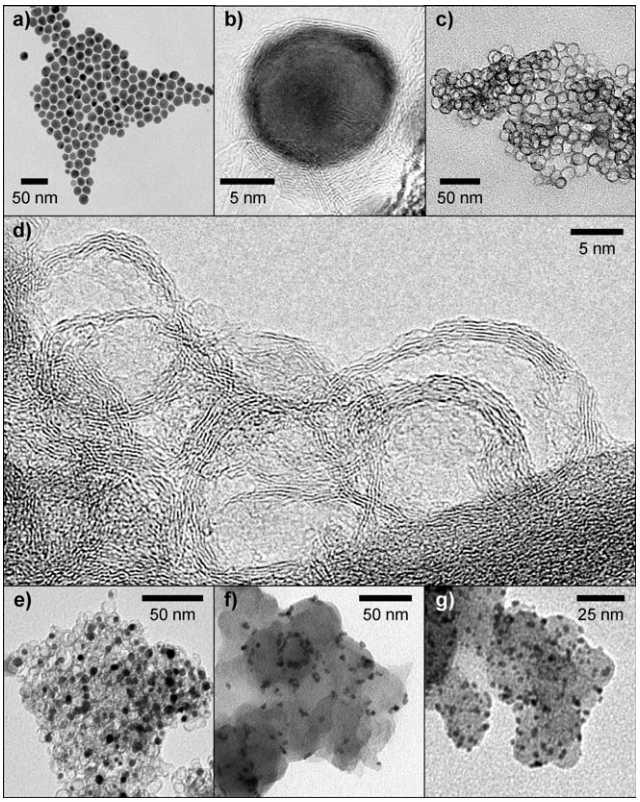

Figure 3. TEM images of a) as-prepared Ni_3C nanoparticles, b) Ni@C produced by thermally-induced phase segregation of the Ni_3C particles, c,d) uniform hollow carbon shells produced by acid leaching of nckel from Ni@C, (e) polyol-deposited 5 wt% Pt/C shell, f) polyol-deposited 5 wt% Pt/Vulcan, and g) commercial ETEK 20% Pt/Vulcan. The HRTEM images in (b) and (d) show the predominant graphitic character of the carbon shells.

ranges from 2.5–3.5 nm, is graphitic, with the (002) basal planes clearly evident in the HRTEM image (Figure 3d).

Figure 3c shows a representative TEM image of the final carbon shells after the nickel core has been etched. The carbon shells are spherical and uniform with diameters of about 20 nm, which is consistent with the size of the Ni_3C NP precursors. A HRTEM image (Figure 3d) confirms the graphitic nature of the hollow carbon shells, along with disordered regions. The HRTEM image also indicates that the thickness of the carbon shells remains close to 2.5 nm, which is consistent with an average thickness of seven graphite layers. Compared to other hollow carbon nanostructures that have been made previously (primarily by pyrolysis routes),[18] these carbide-derived carbon shells tend to be smaller, more dispersible, and significantly more uniform in size and morphology.

The powder XRD pattern of the carbon shells (Figure 2) shows only broad peaks that are attributable to graphite. No nickel peaks are observed by XRD, and nickel is also not observed in EDS data. Nitrogen adsorption measurements of the carbon shells indicate Brunauer–Emmett–Teller (BET) surface areas[19] that range from 525–600 $m^2 g^{-1}$, which is consistent with other highly porous carbon materials. The N_2 adsorption/desorption analysis (Supporting Information, Figure S1) reveals a type IV isotherm that indicates mesoporosity, although micropores are also present. The Barret–Joyner–Halenda (BJH) pore volume[20] (mesopores) is 0.8–0.9 $cm^3 g^{-1}$. The mesopore size distribution is broad, with a maximum centered around 2.5 nm. Analysis using the Horvath–Kawazoe (HK) method[21] indicates micropores of approximately 0.8 nm.

Pt NPs were anchored onto the carbon shell substrates at a loading of 5 wt% Pt by the polyol-mediated reduction of $K_2[PtCl_6]$.[22] Powder XRD data for this sample (Figure 2) matches that expected for a mixture of graphite and nanocrystalline platinum. Scherrer analysis of the XRD data indicates a particle size of approximately 6 nm. This is consistent with the particle size observed by TEM, which was about 2–6 nm. For comparison, Pt NPs were anchored in an analogous way to a commercially available Vulcan XC-72 carbon support, and the size, dispersity, and loading were identical, within the limits of detection (Figure 2 and Figure 3). TEM images for both samples (polyol–Pt-on-C-shells and polyol-Pt-on-Vulcan XC-72), along with commercial ETEK Pt/Vulcan (20% Pt, 3–4 nm Pt NPs), are shown in Figure 3. Each sample contained Pt NPs of approximately the same size. (For a HRTEM image of the Pt/C shell sample, see the Supporting Information, Figure S2.)

Electrochemical hydrogen absorption–desorption and oxygen reduction mass activity for 5% Pt/C shells, 5% Pt/Vulcan, and ETEK 20% Pt/Vulcan were measured with the powders adhered to a glassy-carbon rotating-disc electrode. The hydrogen adsorption–desorption data obtained by cyclic voltammetry (CV) in nitrogen-purged 0.5 M H_2SO_4 show a very high capacitance for the carbon nanoshells containing 5 wt% Pt (Supporting Information, Figure S3). The high capacitance of the Pt/C shell catalysts, which has been observed previously for other high-surface-area carbon materials,[2,3] masked detailed hydrogen adsorption–desorp-

tion features, which are evident for the ETEK 20% Pt/Vulcan control catalyst and for polyol-deposited Pt/Vulcan. The high capacitance measured in CV experiments is likely to be a result of the high surface area of the carbon nanoshells.

The apparent mass activity of the 5% Pt/C shell catalysts as measured in 0.5 M H_2SO_4 with air sparging was approximately 6 mA per mg Pt at 0.6 V versus Ag/AgCl. This apparent mass activity is more than twice that of the ETEK 20% Pt/Vulcan control sample (Figure 4). The results for the

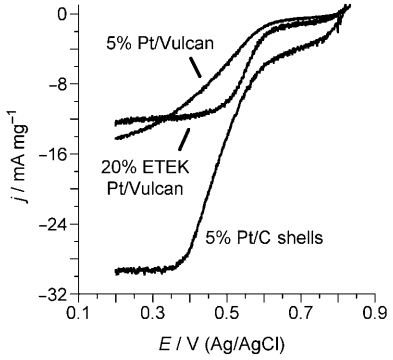

Figure 4. Polarization curves for carbon-supported platinum catalysts in 0.5 M H_2SO_4 at room temperature (normalized to platinum mass), showing a significant increase in ORR current for the 5% Pt/C shell sample.

ETEK control sample agree with previous studies of platinum catalysts in air-sparged H_2SO_4.[23] The apparent mass activity of the 5% Pt/C shells was also greater than that for polyol-deposited 5% Pt/Vulcan. The similar sizes for the E-TEK catalyst and polyol-deposited 5% Pt/Vulcan are consistent with these catalysts having similar intrinsic mass activities. The size of the Pt NPs on the carbon shells is not significantly different than for those on Vulcan carbon. However, the high surface area of the shells and high Pt NP dispersion on the carbon shell support appears to increase the apparent platinum mass activity in the rotating disk experiments.

In conclusion, we have designed and demonstrated a multistep template-based strategy for generating circa 20 nm graphitic carbon shells that are uniform in both size and shape. These novel shells can serve as high-surface-area carbon supports for highly-dispersed Pt NP catalysts, resulting in apparent platinum mass activities for the ORR in 0.5 M H_2SO_4 that are more than twice that of comparable commercial and control catalysts. Given the prevalence of nanostructured carbon materials in many other applications, these carbon shells also have the potential to be generally useful for improving properties and performance in areas beyond catalysis, such as energy storage, environmental remediation, and biomedical detection and analysis.

Experimental Section

Synthesis of Ni_3C: Nickel 2,4-pentanedionate (256 mg, 95%, Alfa Aesar) was dissolved in a mixture of 1-octadecene (8.5 mL, 90%, Alfa Aesar), oleylamine (1 mL, min. 40%, TCI America), and trioctylphosphine (0.5 mL, 90%, Aldrich) in a 100 mL three-neck round-bottom flask equipped with a condenser, thermometer, and magnetic stir bar. The mixture was heated by mantle to 120 °C while periodically evacuating under vacuum and backfilling with argon, then heated to 240 °C under argon and held at that temperature for 1 h. The flask was removed from the heat and allowed to cool to room temperature. An excess of methanol/cyclohexane (3:1) was added, and the nickel nanoparticle product was collected by centrifugation and dried under ambient conditions. This procedure yields 20–30 mg of Ni_3C, but the reagents can be scaled up appropriately to yield 2–3 g with no observable change in particle size or dispersity.

Synthesis of Ni@C: Finely ground Ni_3C powder was placed in a ceramic boat in a quartz tube and heated in an argon-filled tube furnace by raising the temperature to 450 °C over 2.5 h and holding at that temperature for 15 min, followed by cooling under ambient conditions to room temperature.

Synthesis of carbon shells: The Ni@C product was placed in a 40 mL scintillation vial with a magnetic stir bar, and while slowly stirring, 10 mL of concentrated HNO_3 was added very slowly. (***Caution***: this reaction rapidly liberates hazardous gas and heat, and must be performed slowly, in a fume hood, and with appropriate safety precautions). Instead of concentrated HNO_3, 0.5 M HNO_3 can also be used, along with a longer reaction time. After the acid was added, the reaction was allowed to proceed for 1–2 h. The carbon shells were then collected by centrifugation, washed several times with water until the pH of the supernatant was neutral, and finally washed with ethanol.

Synthesis of Pt/C-shells and Pt/Vulcan: Ethylene glycol (10 mL, J.T. Baker) and potassium hexachloroplatinate(IV) (5.7 mg, Alfa Aesar) were placed in a 50 mL Schlenk flask with a magnetic stir bar. The mixture was sonicated for 5 min, placed in a 60 °C oil bath with stirring, and heated with periodic vacuum and argon backfilling cycles until the platinum salt had dissolved (ca. 1 h). The flask was removed from the oil bath and carbon shells (ca. 40 mg) were added to the solution. The flask was returned to the oil bath, which was heated to 110 °C and held for 1 h. After cooling to room temperature, the product was collected by centrifugation and washed with acetone. Pt/Vulcan was made in an analogous manner, except that about 40 mg of MISC Milled Vulcan XC-72 Carbon (E-TEK) was used instead of the C-Shells.

For materials characterization and catalytic testing, see the Supporting Information.

Received: May 27, 2010
Published online: August 18, 2010

Keywords: carbon · mesoporous materials · nanostructures · supported catalysts · template synthesis

[1] J. Lee, J. Kim, T. Hyeon, *Adv. Mater.* **2006**, *18*, 2073.
[2] A. Stein, Z. Wang, M. A. Fierke, *Adv. Mater.* **2009**, *21*, 265.
[3] D. S. Su, R. Schlögl, *ChemSusChem* **2010**, *3*, 136.
[4] X. Yu, S. Ye, *J. Power Sources* **2007**, *172*, 133.
[5] W.-P. Zhou, X. Yang, M. B. Vukmirovic, B. E. Koel, J. Jiao, G. Peng, M. Mavrikakis, R. R. Adzic, *J. Am. Chem. Soc.* **2009**, *131*, 12755.
[6] B. C. H. Steele, A. Heinzel, *Nature* **2001**, *414*, 345.
[7] A. A. Gewirth, M. S. Thorum, *Inorg. Chem.* **2010**, *49*, 3557.
[8] C. Wang, H. Daimon, T. Onodera, T. Koda, S. Sun, *Angew. Chem.* **2008**, *120*, 3644; *Angew. Chem. Int. Ed.* **2008**, *47*, 3588.
[9] B. Lim, M. Jiang, P. H. C. Camargo, E.-C. Cho, J. Tao, X. Lu, Y, Zhu, Y. Xia, *Science* **2009**, *324*, 1302.
[10] J. X. Wang, H. Inada, L. Wu, Y. Zhu, Y. Choi, P. Liu, W.-P. Zhou, R. R. Adzic, *J. Am. Chem. Soc.* **2009**, *131*, 17298.
[11] S. H. Joo, S. J. Choi, I. Oh, J. Kwak, Z. Liu, O. Terasaki, R. Ryoo, *Nature* **2001**, *412*, 169.

[12] G. Yushin, A. Nikitin, Y. Gogotsi, *Carbon Nanomaterials*, CRC, Boca Raton, FL, **2006**, 211.
[13] H. Dai, *Carbon Nanotubes: Synthesis Structure, Properties, and Applications*, Springer, Berlin, **2001**, p. 29.
[14] a) Y. Leng, H. Shao, Y. Wang, M. Suzuki, X. Li, *J. Nanosci. Nanotechnol.* **2006**, *6*, 221; b) Y. Leng, Y. Liu, X. Song, X. Li, *J. Nanosci. Nanotechnol.* **2008**, *8*, 4477; c) Y. Goto, K. Taniguchi, T. Omata, S. Otsuka-Yao-Matsuo, N. Ohashi, S. Ueda, H. Yoshikawa, Y. Yamashita, H. Oohashi, K. Kobayashi, *Chem. Mater.* **2008**, *20*, 4156.
[15] X. Luo, Y. Chen, G.-H. Yue, D.-L. Peng, X. Luo, *J. Alloys Compd.* **2009**, *476*, 864.
[16] Y. Leng, L. Xie, F. Liao, J. Zheng, X. Li, *Thermochim. Acta* **2008**, *473*, 14.
[17] F. J. Maldonado-Hódar, C. Moreno-Castilla, J. Rivera-Utrilla, Y. Hanzawa, Y. Yamada, *Langmuir* **2000**, *16*, 4367.
[18] a) S. Han, Y. Yun, K.-W. Park, Y.-E. Sung, T. Hyeon, *Adv. Mater.* **2003**, *15*, 1922; b) A.-H. Lu, W.-C. Li, N. Matoussevitch, B. Spliethoff, H. Bönnemann, F. Schüth, *Chem. Commun.* **2005**, 98; c) J. N. Wang, L. Zhang, J. J. Niu, F. Yu, Z. M. Sheng, Y. Z. Zhao, H. Chang, C. Pak, *Chem. Mater.* **2007**, *19*, 453.
[19] S. Brunauer, P. H. Emmett, E. Teller, *J. Am. Chem. Soc.* **1938**, *60*, 309.
[20] E. P. Barrett, L. G. Joyner, P. P. Halenda, *J. Am. Chem. Soc.* **1951**, *73*, 373.
[21] F. Rouquerol, J. Rouquerol, K. Sing, *Adsorption by Powders and Porous Solids*, Academic Press, San Diego, **1999**.
[22] J. C. Bauer, X. Chen, Q. Liu, T.-H. Phan, R. E. Schaak, *J. Mater. Chem.* **2008**, *18*, 275.
[23] U. A. Paulus, T. J. Schmidt, H. A. Gasteiger, R. J. Behm, *J. Electroanal. Chem.* **2001**, *495*, 134.

